ation of K^+. Our results complement experiments in which (i) point mutations at several amino acids in a corresponding segment of the S5-S6 loop of the Shaker K^+ channel changed external blockade by TEA (*8*); (ii) several mutations at one amino acid, T449, changed both TEA blockade and inward single channel conductance (*8*); and (iii) a mutation at T441 greatly reduced internal TEA blockade (*20*). Because of the concurrence of the conclusions from point mutation experiments and our experiments with the chimeric channel, it is unlikely that either result is caused by an unintended structural change induced by the mutation. The extensive changes induced by the chimeric exchange are, in any case, not easily explained by a structural effect because three pronounced characteristics of the donor phenotype were transferred nearly unaltered.

Of the 21 amino acids in the transplanted region, there are nine differences between NGK2 and DRK1 and five of them (Fig. 1B) are nonconservative substitutions. Of these, the Q at position 409 of NGK2 corresponding to K382 in DRK1 is especially interesting because on electrostatic grounds it could account for the differences between DRK1 and NGK2 in external TEA blockade and rectification. The neighboring Y at position 407 of NGK2 corresponds to T449 of Shaker, which is known to be important for external TEA blockade and single channel conductance (*8*).

Functional experiments led to the prediction that the pore of voltage-gated ion channels would have dimensions accommodating one or two ions and a few water molecules (*21*). The results with point mutations (*8*) and our results with the chimeric channel indicate that the pore may be determined by a stretch of 21 amino acids. If this region forms an α-helical hairpin it would have a length of about 15 Å, and the 30 Å thick membrane would therefore have to be constricted in the pore region. Another possibility that is more compatible with the membrane thickness is that this stretch of amino acids forms two antiparallel β-strands that could traverse the membrane.

REFERENCES AND NOTES

1. M. Noda *et al.*, *Nature* **320**, 188 (1986).
2. H. R. Guy and P. Seetharamulu, *Proc. Natl. Acad. Sci. U.S.A.* **83**, 508 (1986).
3. R. E. Greenblatt *et al.*, *FEBS Lett.* **193**, 125 (1985).
4. W. A. Catterall, *Science* **242**, 50 (1988).
5. H. R. Guy and F. Conti, *Trends Neurosci.* **13**, 201 (1990).
6. B. L. Tempel *et al.*, *Science* **237**, 770 (1987).
7. R. MacKinnon and C. Miller, *ibid.* **245**, 1382 (1989).
8. R. MacKinnon and G. Yellen, *ibid.* **250**, 276 (1990).
9. C. M. Armstrong and L. Binstock, *J. Gen. Physiol.* **48**, 859 (1965).
10. G. C. Frech, A. M. J. VanDongen, G. Schuster, A. M. Brown, R. H. Joho, *Nature* **340**, 642 (1989).
11. S. Yokoyama *et al.*, *FEBS Lett.* **259**, 37 (1989). The NGK2 clone was isolated from a rat brain cDNA library and is the rat homolog of the NG108 isolate.
12. The BamH I restriction fragment (position 906 and 1516 in the coding region) was excised from DRK1 and subcloned into M13mp19. Silent restriction sites for BspM I (C to A and C to T change at positions 1080 and 1083, respectively) and Stu I (G to A and G to C change at positions 1170 and 1173, respectively) were introduced [J. R. Moorman *et al.*, *Science* **250**, 688 (1990)]. The BamH I fragment was ligated back into DRK1, and the extent of the fragment was sequenced. cRNA run-off transcripts were prepared and microinjected into *Xenopus* oocytes [R. H. Joho *et al.*, *Mol. Brain Res.* **7**, 105 (1990); A. M. J. VanDongen *et al.*, *Neuron* **5**, 433 (1990)]. In oocytes the cRNA for DRK1 directed the expression of whole-cell and single channel currents that were indistinguishable from those for the parent DRK1. NGK2 (*11*) was cloned from a rat brain cDNA library (*10*). In oocytes cRNA directed expression of whole-cell and single channel currents that were identical to those from NG108 cells. The DNA segment in DRK1 corresponding to the region encoding amino acids 364 through 390 was replaced with the DNA segment encoding amino acids 391 through 417 of NGK2. Because the first four and the last two amino acids of the substituted restriction fragment were identical to those of DRK1, the chimeric region actually extended over 21 amino acids. The NGK2 segment to be exchanged was synthesized by the polymerase chain reaction (PCR) technique [H. A. Erlich, Ed., *PCR Technology* (Stockton Press, New York, 1989)] with forward 5′-ATATACCTGCCGGCTTCTGGTGGGCTGTGGT) and reverse (5′-GCACAGGCCTCCCACCAACATCCCAGACCA) primers encoding at their 5′ ends a BspM I and a Stu I site, respectively. The recognition sites were preceded by four extra nucleotides to allow efficient restriction enzyme digestion of the PCR product for cloning into DRK1 that had been cut with BspM I and Stu I. The construct was verified by restriction mapping and sequencing. cRNA run-off transcripts were prepared and microinjected as above.
13. Whole-cell recording from Stage V–VI *Xenopus* oocytes was performed and analyzed as described [A. M. J. VanDongen *et al.*, *Neuron* **5**, 433 (1990)] except that the potential electrode was filled with 120 mM potassium methanesulfonate (MES), 2 mM $MgCl_2$, 10 mM Hepes, and 50 mM TEACl (pH 7.2). TEACl was substituted for NMDGMES in the external solution as necessary. To inject TEA, a pneumatic pressure ejector (Picospritzer II, General Valve Corp.) was connected to the potential electrode. The volume injected was estimated from the volume of the fluid droplet expelled in air with the pipet tip prior to and after penetration of the oocyte [I. Parker and R. Miledi, *Proc. R. Soc. London B* **228**, 307 (1986)]. The volume was always less than 2% of the oocyte volume. Injection of equal amounts of TEA-free vehicle was without effect. The experiments were performed at 21°C. Single channel currents were recorded and analyzed as described [J. R. Moorman *et al.*, *Neuron* **4**, 243 (1990)]. The pipet solution was 120 mM NaCl, 2.5 mM KCl, 2 mM $MgCl_2$, 10 mM Hepes, pH 7.2. A bath solution that depolarized the membrane to 0 mV was used and was 100 mM KCl, 10 mM EGTA, 10 mM Hepes, pH 7.2.
14. C. M. Armstrong. *J. Gen. Physiol.* **58**, 413 (1971).
15. M. Taglialatela *et al.*, manuscript in preparation.
16. E. Koppenhöfer and W. Vogel, *Pfluegers Arch.* **313**, 361 (1969).
17. C. M. Armstrong and B. Hille, *J. Gen. Physiol.* **59**, 388 (1972).
18. S. H. Thompson, *J. Physiol (London)* **265**, 465 (1977).
19. A. Hermann and A. L. F. Gorman, *Neurosci. Lett.* **12**, 87 (1979).
20. G. Yellen, M. Jurman, T. Abramson, R. MacKinnon, *Science* **251**, 939 (1991).
21. B. Hille, *Ionic Channels of Excitable Membrane* (Sinauer, Sunderland, MA, 1984).

22. We thank S. Verma for cloning the rat brain homolog of NGK2, G. Schuster for oocyte management, and D. Witham and J. Breedlove for their secretarial assistance. Supported in part by National Institutes of Health grants NS23877 to A.M.B., NS28407 to R.H.J., and NS08805 to J.A.D., American Heart Association–Texas Affiliate 89R197 to G.E.K., and the Italian National Research Council (CNR) to M.T.

12 December 1990; accepted 22 January 1991

Reshaping the Cortical Motor Map by Unmasking Latent Intracortical Connections

KIMBERLE M. JACOBS AND JOHN P. DONOGHUE

The primary motor cortex (MI) contains a map organized so that contralateral limb or facial movements are elicited by electrical stimulation within separate medial to lateral MI regions. Within hours of a peripheral nerve transection in adult rats, movements represented in neighboring MI areas are evoked from the cortical territory of the affected body part. One potential mechanism for reorganization is that adjacent cortical regions expand when preexisting lateral excitatory connections are unmasked by decreased intracortical inhibition. During pharmacological blockade of cortical inhibition in one part of the MI representation, movements of neighboring representations were evoked by stimulation in adjacent MI areas. These results suggest that intracortical connections form a substrate for reorganization of cortical maps and that inhibitory circuits are critically placed to maintain or readjust the form of cortical motor representations.

ALTHOUGH IT HAS BEEN ARGUED that the MI map is basically stable over time in adult animals (*1*), the possibility that MI continually reorganizes has been recognized since Sherrington's studies (*2*). The details of MI maps vary considerably in size and shape between animals, but the relative location of face, forelimb, and hindlimb areas is one consistent

Center for Neural Science, Box 1953, Brown University, Providence, RI 02912.

feature (*3, 4*). It has been shown that new MI representation patterns emerge after peripheral nerve transections in rats (*4, 5*). Within a few hours after the motor nerve innervating the mystacial vibrissa is transected, movements of body parts normally represented in adjacent motor cortical areas can be evoked by stimulation within the former MI vibrissa area. Thus, it appears that a region of motor cortex modifies its output organization so that one set of cortical neurons influences a new set of muscles. The rapid time course of this reorganization suggests that, rather than growing new connections, existing synaptic connections alter their effectiveness.

One substrate for rapid changes in cortical organization may be the pattern of inhibitory and excitatory connections within the cortex. Relief of inhibition can facilitate the strengthening of synaptic efficacy that occurs after tetanic stimulation within the hippocampus and neocortex (*6, 7*). We propose a model of intracortical connectivity in which the organization of the cortical motor map is regulated by inhibitory local circuit neurons. These neurons use the transmitter γ-aminobutyric acid (GABA) and form the principal inhibitory cell class in cortex. The expression of intracortical excitatory connections between MI output neurons in our model (Fig. 1) is normally weak because intracortical fibers simultaneously activate these GABA neurons. The inhibitory cells then project to nearby pyramidal neurons and rapidly suppress the effectiveness of any excitatory drive from surrounding representations. There is considerable evidence to support the existence of these types of local intracortical connections throughout the cortex (*8*). Although the role of these circuits is unknown, this connectivity pattern may limit the group of cells activated by intracortical stimulation or by natural activity and could serve therefore to define the topographic pattern in MI. If inhibitory circuits are appropriately placed, small adjustments in intracortical inhibition would be sufficient to unmask latent connections and reorganize the MI map. Stimulation at low-current intensities (≤60 μA) in lateral parts of MI in rats typically evokes forelimb movement; mystacial vibrissa movements are evoked from medially adjacent parts of MI (*4*). We tested the prediction of our model that forelimb movements would be evoked from the vibrissa area when inhibitory masking of lateral excitation within the forelimb representation of MI was blocked.

We assessed the effect of inhibition on motor cortical organization in 15 adult rats by monitoring the electromyographic activity (EMG) and movements evoked by intracortical electrical stimulation at sites within MI while inhibition at a remote MI site was locally adjusted. Initial electrical stimulation mapping was used to identify the general pattern of topography in MI and the boundary between the forelimb and vibrissa areas (*9*). The effectiveness of local inhibitory circuits was reduced by iontophoretically releasing the GABA antagonist, (−)bicuculline methobromide (bic), at a site within the MI forelimb area (Fig. 1). One site within the vibrissa representation from which stimulation before bic application elicited vibrissa, but not forelimb movements, was chosen as the site to be tested (vib test site) at regular intervals before and after bic release. After 5 to 65 min (mean ± SEM, 26.6 ± 4.5; n = 15) of bic ejection within the forelimb representation, forelimb EMG was evoked by stimulation at the vib test site (Fig. 2B). Thus, after bic application, forelimb as well as vibrissa musculature was activated by electrical stimulation at the vib test site, now a "modified" vib site. The ability of the vib test site to shift from activating only vibrissa movements to eliciting both forelimb and vibrissa movements could be repeatedly demonstrated within the same animal (*10*) (Fig. 3). After termination of the bic ejection (15 to 195 min, mean ± SEM, 68.8 ± 14.2), stimulation at the vib test site no longer elicited forelimb movements (Figs. 2 and 3). We do not know if the persistence of the shift is a result of the slow clearance of bic from the forelimb application site, or is due to a long-lasting change in the strength of excitatory connections, as has been described for other pathways within neocortex (*7, 11*).

One explanation of our results is that bic generally increased cortical excitability. We do not believe this to be true for two reasons. First, bic spread only to a restricted part of the MI. We estimated the extent of inhibitory blockade by measuring the spread of iontophoretically applied [^{3}H]bicuculline methyl chloride (*12*) in one case. Autoradiograms of unfixed coronal sections through the applications site showed a radial spread of radioactive label. The results suggested that there was very little, if any, direct effect of bic beyond 660 μm from the application site (*13*). The second reason that we believe that there was not an overall increase in

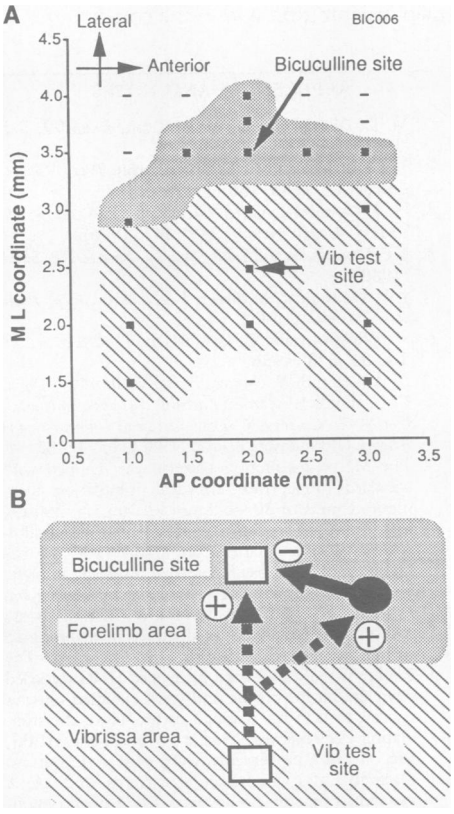

Fig. 1. Cortical surface map of MI from case BIC006, illustrating (**A**) the location of stimulating and bic electrodes and (**B**) arrangement of hypothetical extant connections. (A) Each square represents a site from which movement of either the forelimb (shaded region) or vibrissa (diagonal hatching) was evoked at the lowest current intensities. Dashed lines represent sites from which stimulation did not evoke movements at currents ≤60 μA. (B) Schema of intracortical connections in which excitatory effects are limited to the MI vibrissa area. Excitation from vibrissa area (dashed line) activates neurons in the forelimb area, but nearly simultaneous disynaptic inhibition (black cell and line) reduces the effectiveness of the vibrissa area input to the forelimb area. ML, medial-lateral; AP, anterior-posterior.

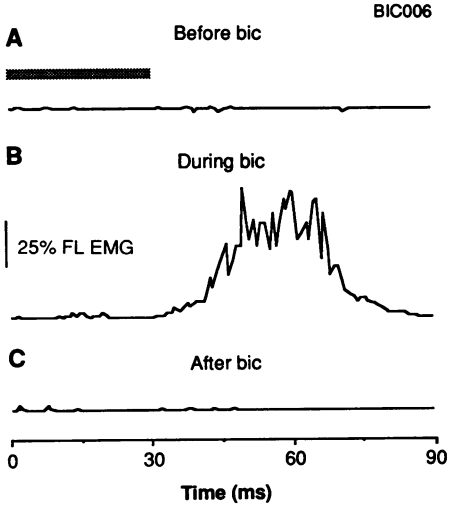

Fig. 2. Forelimb EMG evoked by stimulation in the MI vibrissa area during remote bic application. (**A**) Biceps EMG (rectified, ten-trial average) elicited by stimulation at a normal vibrissa site (vib test site). Stimulus train occurs during time indicated by horizontal bar. (**B**) Forelimb EMG (FL EMG) elicited by stimulation at same vib test site as in (A) after 65 min of bic application. (**C**) Forelimb EMG elicited by stimulation at same site as in (A) and (B) 125 min after termination of bic application. All values normalized to largest normal forelimb EMG obtained in this case.

cortical excitability is that thresholds to evoke vibrissa movement at the vib test site were not lowered by bic application (*14*).

Our experiments show that reductions in local inhibition can temporarily rearrange the relation between an area of MI and the muscles. In other experiments, we excluded the possibility that agents that increase excitation would be similarly effective in producing reorganization. We tested this in three cases in which we substituted bic with either acetylcholine chloride (ACh) or sodium glutamate while using the same iontophoretic application and stimulation mapping procedures (*15*). Neither ACh nor glutamate application for up to 95 min altered the movements evoked by stimulation at the vib test site (Fig. 3); in these cases an average of 19.2 min of bic application (range, 5 to 45 min) was sufficient to modify the movements evoked at this same vib test site. These amounts of glutamate or ACh applications excite layer V neurons (*16–19*). Thus, this expansion of one representation into another is much more sensitive to adjustments in inhibition than to a generalized increase in excitation.

The effects of reduced inhibition were examined over a broader extent of MI by stimulating several of the same MI sites before and after bic application in 6 of the 15 rats. After bic application, forelimb EMG could be evoked at many sites within the vibrissa representation (Fig. 4). At some of the modified sites in the vibrissa region (strongly modified sites), forelimb muscle activity was evoked at lower current intensities than those required to evoke vibrissa movement. The location of these sites was not simply correlated to the distance between the bic application and test stimulation sites. After the bic application, some vib test sites up to 3 mm away were strongly modified by the bic, but at other sites closer to the bic application, vibrissa movement was still evoked at the lowest stimulating currents. This irregularity in the pattern of modified sites may reflect an underlying pattern of nonuniform connectivity within MI.

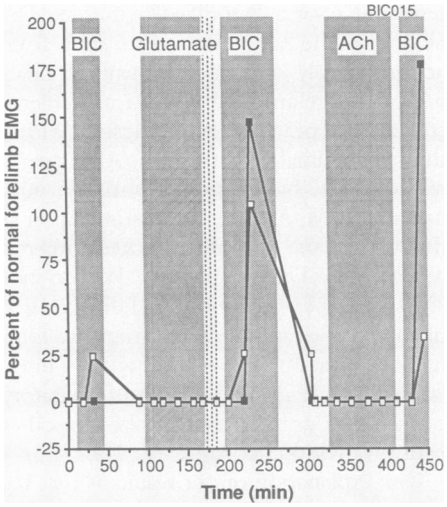

Fig. 3. Change in forelimb EMG activity over time, during iontophoretic application of excitatory or disinhibitory agents. Each point represents rectified, averaged EMG activity, integrated over 100 ms following stimulation to the cortical vib test site (background EMG subtracted). The EMG was recorded from biceps (■) and wrist extensor (□) muscles. Shaded columns represent the duration of application of the bic, ACh, or glutamate. Bic was applied three times, at 50, 50, and 150 nA, respectively; glutamate was applied at 25 nA initially, then the current was increased to 50 nA (vertical dashed lines); ACh was applied at 50 nA. Both glutamate and ACh were without effect. The stimulation and bic application sites were 2 mm apart.

The modifications that occur after relief of inhibition suggest that an intracortical connectional substrate is appropriately placed to permit flexible associations between MI and the somatic musculature. This role for inhibitory circuits should generalize across cortex, since the connectivity patterns that underlie this phenomenon are not peculiar to MI; similar circuits may participate in reorganization of cortical maps in other parts of neocortex. Evidence for the implementation of this mechanism would require changes in intracortical inhibition under circumstances where cortical reorganization is observed. Several reports have shown that GABA markers are changed within the neocortex after peripheral lesions or sensory deprivation (*20*). Modification of the strength of inhibition after electrical stimulation also occurs in the hippocampus (*21, 22*), which contains similar excitatory and inhibitory arrangements. That these changes can persist (*22*) suggests that inhibitory synapses may undergo long-term alterations in efficacy. Temporary alterations in the strength of inhibition could also serve as a gate, allowing the enhancement of excitatory synaptic strength during conditions of lowered inhibition (*7, 23*).

Pharmacologically produced adjustments in the inhibitory circuitry shown here appear to produce functional reorganization similar to that observed after nerve lesions. Naturally occurring alterations in activity could, in a more subtle form, reshape cortical circuits during learning. These same mechanisms may lead to the uncontrolled spread of activity, as occurs during epileptic seizures. Small changes in GABA activity occurring throughout the cortex lead quickly to spread of activity to horizontally distant sites in the cortex (*24*). More local changes in GABA activity, such as those occurring after certain patterns of activation, may initiate the types of recovery of function seen after brain damage due to stroke or ischemic injury. Further, local changes in GABA activity may lead to temporary associations between adjacent cell groups, enabling reorganization. These results suggest that the architecture of inhibitory circuits is crucial to dynamic processes and map organization within the cortex.

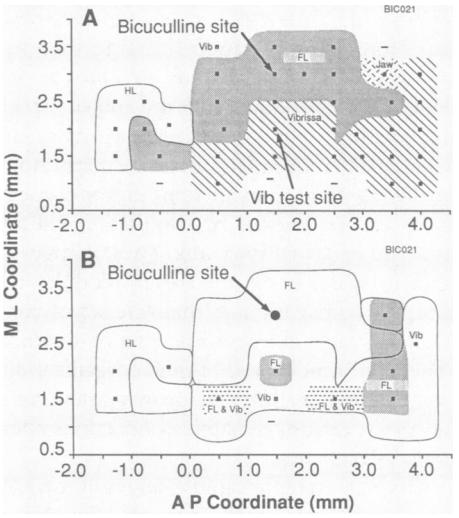

Fig. 4. Pattern of reorganization after bic application. (**A**) Map of movements evoked before bic application. FL, forelimb area; HL, hindlimb; Vib, vibrissa area; FL & Vib, both movements evoked at threshold stimulation. (**B**) Effects obtained at several sites during bic application sufficient to yield forelimb EMG from the initial vib test site. Outlines mark original borders; modified sites are shaded. The total amount of potential expansion appears to be constrained, since at no time did noncontiguous representations expand into each other. These limits are presumably set by the connectivity patterns within MI.

REFERENCES AND NOTES

1. M. D. Craggs and D. N. Rushton, *Brain* **99**, 575 (1976).
2. T. G. Brown and C. S. Sherrington, *Proc. R. Soc. London Ser. B* **85**, 250 (1912).
3. H. J. Gould III, C. G. Cusick, T. P. Pons, J. H. Kaas, *J. Comp. Neurol.* **247**, 297 (1986).
4. J. P. Donoghue and J. N. Sanes, *J. Neurosci.* **8**, 3221 (1988).
5. J. P. Donoghue, S. Suner, J. N. Sanes, *Exp. Brain Res.* **79**, 492 (1990).
6. H. Wigstrom and B. Gustafsson, *J. Physiol. (London)* **81**, 228 (1986).
7. A. Artola and W. Singer, *Nature* **330**, 649 (1987).
8. E. L. White, in *Cortical Circuits: Synaptic Organization of the Cerebral Cortex: Structure, Function, and Theory* (Birkhauser, Boston, 1989), pp. 46–82.
9. The MI representation pattern was mapped with standard intracortical electrical stimulation techniques (trains of 30-ms duration, 300 Hz, 200-μs-long monophasic, cathodal pulses) in 15 adult albino rats during ketamine anesthesia (100 mg per kilogram of body weight, intraperitoneally initially, with 10-mg intramuscular supplemental doses given as necessary). Initially, the location of the vibrissa and forelimb MI areas was identified by mapping 11 to 52 sites spaced 250 to 500 μm apart. The forelimb area was defined by evoked EMG recorded from the biceps brachii and wrist extensor muscles contralateral to the mapped cortex. Next, the stimulating electrode was fixed at a vibrissa site. At this site, vibrissa movements were observed, but no forelimb EMG was evoked at currents ≤60 μA. A glass micropipette (tip diameter 1 to 2 μm) contain-

ing 10 mM bic was placed within the forelimb area, 0.5 to 2.0 mm lateral to the stimulating electrode at a depth of 1.8 mm (layer V). In some experiments a glass multibarrelled micropipette was used for the separate application of bic, ACh, or glutamate. The bic was ejected continuously (50 to 150 nA) at this forelimb site for 7 to 80 min, while movements and EMG evoked by stimulating at the vib test site were recorded at 5- to 15-min intervals.
10. In 12 of the 15 rats, multiple bic applications were made. Second and third applications were made only after the shift was no longer observed. Each application produced the same reorganization.
11. A. Iriki *et al.*, *Science* **245**, 1385 (1989).
12. We applied 0.3 μM (−)[^{3}H]bicuculline methyl chloride through our usual glass pipettes with +5 nA for 2 hours.
13. Sections of unfixed tissue were exposed to autoradiographic film and then developed. Radioactive labeling was measured by a computer-based densitometer. The decrease in labeling density from the center of the application site fit a Gaussian distribution reaching two standard deviations below the peak value 600 μm from the ejection center.
14. Threshold ± SEM for vibrissa movement were 28.1 ± 2.6 μA, n = 43, before and 33.3 ± 2.2 μA, n = 65 (not significant, $P > 0.05$, t test), after bic application.
15. Acetylcholine chloride (0.5 M) was applied with currents of 50 to 150 nA and sodium glutamate (0.5 M) was applied with 25 to 150 nA.
16. R. Metherate, N. Tremblay, R. W. Dykes, *J. Neurophysiol.* **59**, 1231 (1988).
17. K. Krnjevic and J. W. Phillis, *J. Physiol. (London)* **166**, 296 (1963).
18. J. P. Donoghue and K. L. Carroll, *Brain Res.* **408**, 367 (1987).
19. The marked increase in discharge rate of layer V neurons during ACh or glutamate application is the measure of a general increase in excitability described here.
20. N. D. Akhtar and P. N. Land, *Neurosci. Abstr.* **13**, 77 (1987); S. H. Hendry and E. G. Jones, *Nature* **320**, 750 (1986); E. Welker, E. Soriano, H. van der Loos, *Exp. Brain Res.* **74**, 441 (1989).
21. M. McCarren and B. E. Alger, *J. Neurophysiol.* **53**, 557 (1985).
22. A. Stelzer, N. T. Slater, G. T. Bruggencate, *Nature* **326**, 698 (1987).
23. H. Wigstrom and B. Gustafsson, *Acta Physiol. Scand.* **125**, 159 (1985).
24. Y. Chagnac-Amitai and B. W. Connors, *J. Neurophysiol.* **61**, 747 (1989).
25. This work was supported by March of Dimes grant 1-1169 and NIH grants NS22517 and NS25074.

30 July 1990; accepted 28 November 1990

D1 Dopamine Receptors in Prefrontal Cortex: Involvement in Working Memory

TOSHIYUKI SAWAGUCHI AND PATRICIA S. GOLDMAN-RAKIC

The prefrontal cortex is involved in the cognitive process of working memory. Local injections of SCH23390 and SCH39166, selective antagonists of the D1 dopamine receptor, into the prefrontal cortex of rhesus monkeys induced errors and increased latency in performance on an oculomotor task that required memory-guided saccades. The deficit was dose-dependent and sensitive to the duration of the delay period. These D1 antagonists had no effect on performance in a control task requiring visually guided saccades, indicating that sensory and motor functions were unaltered. Thus, D1 dopamine receptors play a selective role in the mnemonic, predictive functions of the primate prefrontal cortex.

IN NONHUMAN PRIMATES, THE PREfrontal cortex (PFC), in particular its dorsolateral region, is critical for the cognitive process of working memory (*1*). Several lines of research suggest that dopamine (DA) may influence this process. The concentration of DA in the PFC is among the highest in all cortical areas in monkeys (*2*), and both DA-containing fibers and DA receptors are prominent in the primate PFC (*3, 4*). Local depletion of DA in the PFC of monkeys induces impairment in tasks that require delayed response (*5*), and neuronal activity related to delayed response performance is augmented by iontophoretically applied DA (*6*). These findings suggest that DA receptors may be involved in the mnemonic processes of the PFC.

There are two types of DA receptors in the central nervous system, D1 and D2 receptors (7); the PFC of primates, including humans, contains a high level of D1 receptors (*4, 8, 9*) and a relatively low or negligible level of D2 receptors (*4, 9, 10*). These findings imply that the D1 receptors are likely to be involved in the mnemonic process mediated by the PFC, but direct evidence is lacking. This hypothesis can now be directly tested by the use of potent D1 antagonists, SCH23390 (*11*) and SCH39166 (*12*), in combination with sensitive behavioral paradigms for assessing working memory.

We used an oculomotor delayed-response (ODR) task in which animals were trained to fixate a central spot on a cathode-ray tube while a visual cue was presented briefly in one of several (6 to 22) locations in the visual field. The cue then disappeared, and after a 1.5- to 6-s delay the animal was required to make a memory-guided saccade to where the target had been presented seconds before. Therefore, to achieve criterion performance on the ODR task the animal had to remember visuospatial data in order to make the correct response at the end of the delay. To distinguish a deficit in mnemonic function from deficits in eye movements or sensory perception, we used a control procedure in which the target remained on during the delay period and the subject made a sensory-guided saccade to the target. Neuronal activity in the dorsolateral PFC of monkeys is involved in the ODR task (*13*), and lesions of the dorsolateral PFC induce deficits in the memory-guided saccades required by the task (*14*). However, to examine the role of neurotransmitters or receptors on specified cortical functions, a method of targeting specific brain regions was required. Therefore, we combined the ODR paradigm with the intracerebral injection of SCH23390 and SCH39166 and now report that the activation of D1 receptors plays a critical role in the mnemonic process mediated by the primate PFC.

Three rhesus monkeys (T, J, and N) were trained in the ODR and control tasks (*15*).

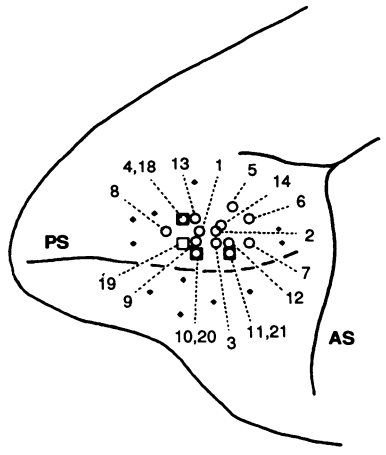

Fig. 1. Injection sites of SCH23390 and SCH39166 in two of the monkeys illustrated on a lateral view of the left PFC. The sites were reconstructed in reference to cortical sulci. Data on injection sites in one monkey, N, that has not yet been killed are not included. However, the effective sites in this monkey are distributed in the same region on the basis of the position of the cylinder and the coordinates of the micromanipulator used for injections; ○, effective sites of SCH23390 on ODR performance; □, effective sites of SCH39166 on ODR performance; ■, ineffective sites with either drug. The number of the injection site in Fig. 1 corresponds to the injection site shown in Table 1. PS, principal sulcus; AS, arcuate sulcus. Injections were placed 2 to 4 mm deep to the dural surface; no sites were located within the banks of the principal sulcus.

Section of Neurobiology, Yale University School of Medicine, New Haven, CT 06510.